



PERGAMON

Available online at www.sciencedirect.com

SCIENCE @ DIRECT®

Vision Research 43 (2003) 2125–2132

Vision
Research

www.elsevier.com/locate/visres

Sampling efficiency and internal noise for motion detection, discrimination, and summation

William A. Simpson^{a,*}, Helle K. Falkenberg^b, Velitchko Manahilov^b

^a SMART–DRDC Toronto, 1133 Sheppard Avenue West, P.O. Box 2000, Toronto, Ont., Canada M3M 3B9

^b Vision Sciences Department, Glasgow Caledonian University, Cowcaddens Road, Glasgow G4 0BA, UK

Received 2 December 2002

Abstract

By comparing real observers to an ideal observer, previous studies have found that the detection of static patterns is limited by internal noise and by imperfect sampling efficiency. We developed and applied ideal observer models for the detection, discrimination, and summation of oppositely drifting gratings in Gaussian white noise. The three tasks share a common source of internal noise. The sampling efficiencies were on the order of 1–2% except for much lower efficiency in direction discrimination for faster moving gratings. The efficiency of direction discrimination relative to detection systematically declines as the speed is increased from 1 to 6 Hz. These results suggest that observers use mismatched filters tuned to slow speeds regardless of the signal speed. Human visual motion sensing appears to use distorted representations of the incoming signals, and this distortion is a major limitation to visual performance.

© 2003 Elsevier Ltd. All rights reserved.

Keywords: Visual motion perception; Motion detection; Motion discrimination; Ideal observer

1. Introduction

Important insights into the limits of visual detection of simple patterns have been gained by comparing the performance of human observers to that of an ideal observer who extracts all the information from the stimuli. Previous studies on the detection of stationary gratings have shown that there are two distinct limiting factors (Burgess, Wagner, Jennings, & Barlow, 1981; Legge, Kersten, & Burgess, 1987; Pelli, 1990; Pelli & Farrell, 1999). Firstly, humans behave as though their visual systems add extra noise to the stimuli. Secondly, they waste the energy in the delivered stimulus—they have low sampling efficiency. Ideal observers cross-correlate the signal they expect to receive with the noisy delivered stimulus. This is a template-matching procedure. One source of low sampling efficiency would be the use of a template that poorly matches the signal.

The aim of this paper is to develop and apply ideal observer models for three classical motion tasks: detection of a drifting grating, discrimination of the direction

of oppositely drifting gratings, and detection of the sum of two gratings drifting in opposite directions. Previous studies have used noiseless displays (Dobkins & Teller, 1996; Levinson & Sekuler, 1975; Stromeyer, Madsen, Klein, & Zeevi, 1978; Thiele, Dobkins, & Albright, 2000; Watson, Thompson, Murphy, & Nachmias, 1980). By adding Gaussian white noise we can measure the internal noise and sampling efficiency.

The ideal observer will detect a drifting grating by cross-correlating the noisy stimulus with a template of the signal. For example if the task is to detect a grating drifting upwards at 1 Hz, the ideal observer will use the spatiotemporal template shown in the upper right corner of Fig. 1. Previous psychophysical evidence (Burr, Ross, & Morrone, 1986; Reisbeck & Gegenfurtner, 1999; Simpson & Manahilov, 2001; Watson & Turano, 1995) points to the existence of such oriented or inseparable spatiotemporal filters in the visual system, and some V1 simple cells are known to behave in this way (DeAngelis, Ohzawa, & Freeman, 1993a, 1993b; Hamilton, Albrecht, & Geisler, 1989; McLean & Palmer, 1989, 1994; McLean, Raab, & Palmer, 1994; Reid, Victor, & Shapley, 1997). As we will show in detail in the next section, the ideal observer's performance in the simple detection task depends only on the energy of the signal

* Corresponding author. Tel.: +1-416-635-2000; fax: +1-416-635-2013.

E-mail address: william.simpson@drdc-rddc.gc.ca (W.A. Simpson).

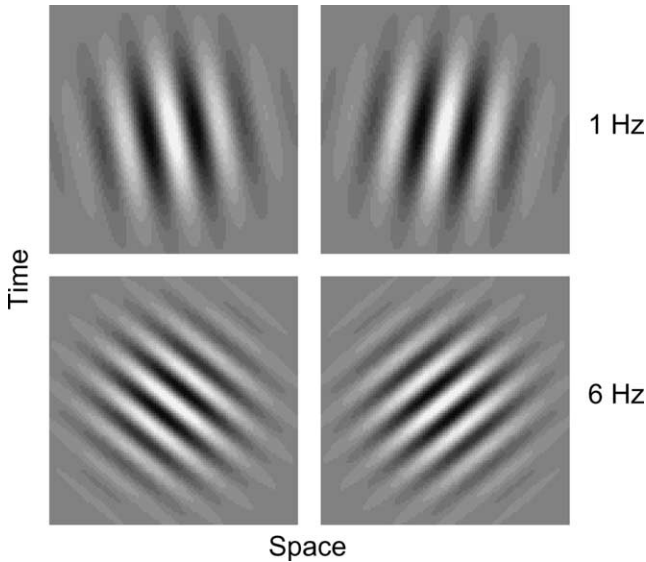


Fig. 1. Space–time plots of Gaussian-windowed horizontal gratings drifting at 1 and 6 Hz. The space axis represents vertical position and so the left panels show downwards motion and the right panels show upwards motion. The 1 Hz Gabors have similar orientations in space–time and have a correlation of 0.77; the 6 Hz Gabors are normal to each other and have a correlation of zero.

and on the noise level. We will measure the noise added internally by human observers and we will measure their sampling efficiency.

For direction discrimination the ideal observer uses a pair of oriented spatiotemporal filters tuned to the two opposite directions of motion to be discriminated (Fig. 1). If the filter corresponding to upwards motion produces the larger cross-correlation with the stimulus, then the observer will decide that upwards motion had been presented, and otherwise the observer will decide that downwards motion had been presented. For simple detection, performance depends only on signal energy and the noise level; in direction discrimination the performance also depends on how similar the two signals being discriminated are. In Fig. 1 space–time diagrams of upwards and downwards drifting Gabors are shown. In a space–time diagram, slowly moving gratings are close to vertical and quickly moving gratings are angled away from vertical. The top pair of gratings move at 1 Hz and are almost vertical in space–time. These two spatiotemporal patterns are highly similar. The similarity is measured by the correlation ρ , which equals 0.77 for these signals. As one might expect, the ideal observer has a hard time discriminating such similar signals. On the other hand, such similar signals are easily summed since the performance of the ideal observer for the summation task also depends on ρ . The bottom pair of gratings in Fig. 1 move at 6 Hz. The spatiotemporal patterns are almost at right angles to one another, signifying a correlation close to zero. These signals will be easy to discriminate but their sum will be hard to detect.

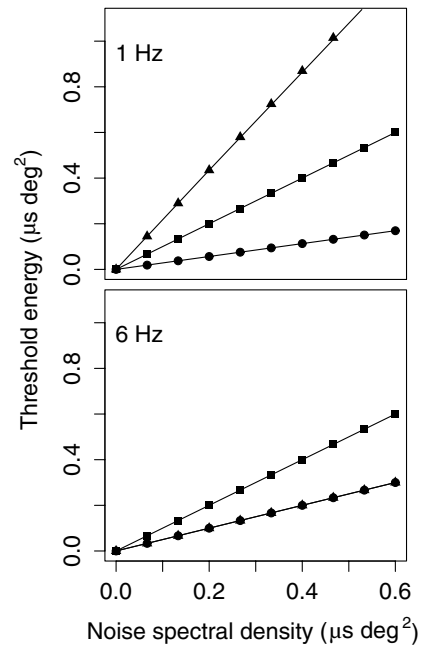


Fig. 2. Energy thresholds as a function of noise spectral density for an ideal observer in detection of a drifting grating (squares), discrimination of motion direction (triangles), and summation of a pair of oppositely drifting gratings (circles). For a speed of 1 Hz, the signals are highly correlated, making discrimination hard and summation easy. At 6 Hz, the signals are uncorrelated, making discrimination much easier and summation somewhat harder.

Fig. 2 shows how the ideal observer's energy thresholds depend on the external noise level and on the correlation between the signals. The energy thresholds for simple detection (squares) rise linearly with the external noise level, and the slope of this line does not change with the signal speed. Thus the reader may use the simple detection function in Fig. 2 as a baseline to see the effect of speed on summation and discrimination. Now consider summation (circles). As the speed increases from 1 to 6 Hz, the slope of the summation curve increases. The increased slope means that summation is poorer at higher frequencies. The reason for this, as we saw in Fig. 1, is that the faster moving gratings drifting in opposite directions have a low cross-correlation—they are dissimilar and thus sum poorly. The pattern is reversed for direction discrimination (triangles): the slope of the function is dramatically reduced as the speed rises from 1 to 6 Hz. The discrimination function pivots from lying above the detection function to lying below it. The faster moving gratings are highly dissimilar and thus are readily discriminated. The overall pattern for the ideal observer is that when the speed is increased discrimination becomes better and summation becomes poorer. If humans behave like an ideal observer, we expect their data to conform to this pattern. We will manipulate the speeds of the signals to see how human performance differs from that of an ideal cross-correlator.

2. Ideal observers

In the experiments we will discuss there are three signals delivered to the observer: s_0 is a blank having zero contrast, s_1 is an upwards drifting Gabor patch, and s_2 is a downwards drifting Gabor. These signals are hidden by added Gaussian white noise with zero mean and power spectral density N_e . In the three experiments the signals are presented in different ways.

2.1. Detection of drifting grating

On each trial the observer receives either s_0 or s_1 and the observer must decide which signal was delivered. The ideal observer cross-correlates the received noisy waveform with a representation of the drifting grating (Fig. 1). The observer's performance (Whalen, 1971, pp. 156–163) is

$$d' = \sqrt{\frac{\iiint (s_1 - s_0)^2 dx dy dt}{N_e}}.$$

The blank has a contrast of zero and obviously has no energy, and the grating has energy $E_1 = \iiint s_1^2 dx dy dt$. Thus

$$d' = \sqrt{\frac{E_1}{N_e}}.$$

If the signal were the downwards drifting Gabor s_2 then we would substitute E_2 for E_1 . Previous experiments have suggested that real observers differ from the ideal in that they add internal noise with power spectral density N_i and have subunity sampling efficiency k . This gives

$$d' = \sqrt{\frac{kE_1}{N_e + N_i}}.$$

In our experiments we will be measuring the energy detection threshold E_t , which is the energy required to give a performance of $d' = 1$. Therefore

$$E_t = \frac{N_e + N_i}{k}. \quad (1)$$

If we increase the external noise power spectral density we expect the energy threshold to increase linearly. The slope is $1/k$, revealing the sampling efficiency; the x -intercept is $-N_i$, revealing the internal noise.

2.2. Direction discrimination of oppositely drifting gratings

The observer receives one of the two oppositely drifting gratings s_1 or s_2 embedded in Gaussian white noise. The task is to decide which signal was delivered. The optimal way to make the decision is by cross-correlating the noisy delivered stimuli with the two signals;

whichever signal produces the larger cross-correlation is the one judged to be present. The performance is

$$d' = \sqrt{\frac{\iiint (s_2 - s_1)^2 dx dy dt}{N_e}}.$$

If we expand the numerator we have

$$\iiint (s_1^2 + s_2^2 - 2s_1s_2) dx dy dt.$$

We have defined E_1 and E_2 previously as the integrated squared contrast of the signals. Whalen defines the correlation between the signals ρ as

$$\rho = \frac{2 \iiint s_1s_2 dx dy dt}{E_1 + E_2},$$

so substituting E_1 , E_2 , and ρ we have

$$d' = \sqrt{\frac{E_1 + E_2 - \rho(E_1 + E_2)}{N_e}}.$$

Since the energies of the drifting gratings are equal in our experiments let us replace E_1 and E_2 with the symbol E , giving

$$d' = \sqrt{\frac{2E(1 - \rho)}{N_e}}.$$

For a nonideal observer we add internal noise and subunity sampling efficiency,

$$d' = \sqrt{\frac{2kE(1 - \rho)}{N_e + N_i}}.$$

In terms of threshold (at $d' = 1$) we have

$$E_t = \frac{N_e + N_i}{2k(1 - \rho)}. \quad (2)$$

Again the energy threshold is predicted to be a linear function of the noise level. The slope depends both on the similarity of the two signals being discriminated and on the sampling efficiency. The x -intercept reveals the internal noise.

2.3. Detection of sum of oppositely drifting gratings

The observer receives either the blank signal s_0 or the sum of the two oppositely drifting gratings $s_1 + s_2$ embedded in noise. The performance of a cross-correlator is

$$\begin{aligned} d' &= \sqrt{\frac{\iiint ([s_1 + s_2] - s_0)^2 dx dy dt}{N_e}} \\ &= \sqrt{\frac{\iiint (s_1 + s_2)^2 dx dy dt}{N_e}}. \end{aligned}$$

Substituting E and ρ we have

$$d' = \sqrt{\frac{2E(1 + \rho)}{N_e}}$$

For the nonideal observer,

$$d' = \sqrt{\frac{2kE(1 + \rho)}{N_e + N_i}}$$

and in terms of threshold we have

$$E_t = \frac{N_e + N_i}{2k(1 + \rho)}. \quad (3)$$

The energy threshold is predicted to rise linearly with the noise level. The slope depends both on the similarity of the two superimposed signals and on the sampling efficiency. The x -intercept reveals the internal noise.

3. Methods

Stimuli were generated by a computer and presented on a CRT monitor (Iiyama Vision Master Pro 450, 640×480 pixels) at a viewing distance of 100 cm. The RGB outputs were combined electronically (Pelli & Zhang, 1991) and an optimum linearized palette of 256 luminances (out of 4096) was used. The stimuli were drifting or flickering horizontal sinewave gratings windowed by a spatiotemporal Gaussian (Gabor patch). The drift speed was either 1 or 6 Hz (up or down) in the first experiment; several temporal frequencies were used in the second experiment. The spatial frequencies used were generally in the range of 1–2 c/deg because it is known that the motion system is more sensitive to lower spatial frequencies. Watson and Turano (1995) found a plateau in sensitivity to drifting gratings having spatial frequencies between 2 and 4 c/deg. In the first experiment (data shown in Fig. 3) the spatial frequency was 1 c/deg. In the second phase of the first experiment (data shown in Fig. 4) the spatial frequency was 2 c/deg for HF and KF but 8 c/deg for WS. The higher spatial frequency was used for WS to allow us to see if the pattern of results changed with higher spatial frequencies preferred by putative “sustained” channels. The same spatial frequencies were used for the second experiment (data shown in Fig. 5) where we examined a range of temporal frequencies.

The duration and diameter of the Gabor patch (defined as 5 standard deviations of the Gaussian window) were 333 ms and 5 deg respectively. A grey area 16.8 deg wide and 12.6 deg high at the mean luminance of 30 cd/m² surrounded the Gabor patch. A central fixation mark was always provided. The stimuli were constructed as movies consisting of 20 frames. The refresh rate of the monitor was 120 Hz; each movie frame was displayed for two screen refreshes. In the first experiment dynamic Gaussian white noise was added to the stimulus. This

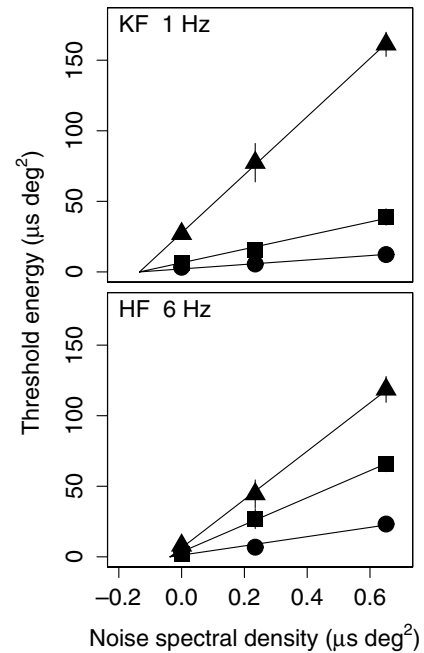


Fig. 3. Threshold energy for detecting an upwards drifting grating (squares), for discriminating an upwards from a downwards drifting grating (triangles), and for detecting the sum of an upwards and downwards drifting grating (circles) plotted as a function of the power spectral density of the added Gaussian white noise. Each point is the mean of 4 threshold measurements for observer KF and 3 for HF; standard errors are shown. The data are for a 1 c/deg Gabor drifting at the speeds shown. The lines are least squares fits of a nonideal cross-correlator model with a source of internal noise common to all the tasks but different sampling efficiencies for each task.

noise was generated by a multiply-with-carry generator (Marsaglia, 1994) in combination with the polar method; it was clipped at ± 2.5 standard deviations.

In the detection experiment the observer decided if an upwards drifting Gabor or a blank was presented. In the discrimination experiment the observer decided whether an upwards or a downwards drifting Gabor had been presented. In the summation experiment the observer decided whether the sum of upwards and downwards drifting gratings (counterphase flickering grating) or a blank had been presented. The different conditions were run in random order. The contrast on each trial was placed according to a staircase procedure (Levitt, 1971). The thresholds were calculated by fitting the nonideal observer psychometric functions to the data by the method of maximum likelihood. The nonideal observer psychometric functions have been presented here in terms of d' . In terms of proportion “yes” judgements, the psychometric function is a cumulative normal distribution whose slope is related to d' and whose sideways shift is related to the criterion.

In the first experiment each plotted threshold is the mean of 4 blocks of 60 trials (for subject HF in Fig. 3 the plotted threshold is the mean of 3 blocks). In the second experiment 3 blocks of trials were used. For the sum-

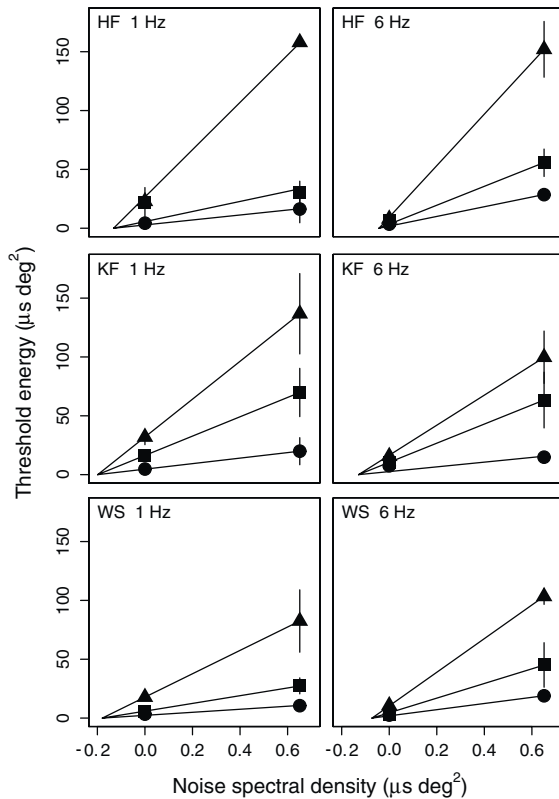


Fig. 4. Threshold energy for detecting an upwards drifting grating (squares), for discriminating an upwards from a downwards drifting grating (triangles), and for detecting the sum of an upwards and downwards drifting grating (circles) plotted as a function of the power spectral density of the added Gaussian white noise. Each point is the mean of 4 threshold measurements; standard errors are shown. The spatial frequency was 2 c/deg for HF and KF and 8 c/deg for WS; the drift speeds were 1 and 6 Hz. The lines are least squares fits of a nonideal cross-correlator model with a source of internal noise common to all the tasks but different sampling efficiencies for each task.

mation experiment the threshold we report is that of one of the two drifting components (Thiele et al., 2000; Watson et al., 1980). The energies and cross-correlations of the stimuli were calculated numerically using the actual stimulus sequences.

4. Results and discussion

In the first experiment we varied the external noise level and measured the threshold energy for detecting an upwards drifting grating, for discriminating upwards from downwards drifting gratings, and for detecting the sum of oppositely drifting gratings. Fig. 3 shows the energy threshold as a function of external noise level for two observers. The spatial frequency was 1 c/deg and the temporal frequency was 1 Hz for KF and 6 Hz for HF. For each of the three tasks we predicted that the data should fall on a line, and that is the pattern shown in Fig. 3.

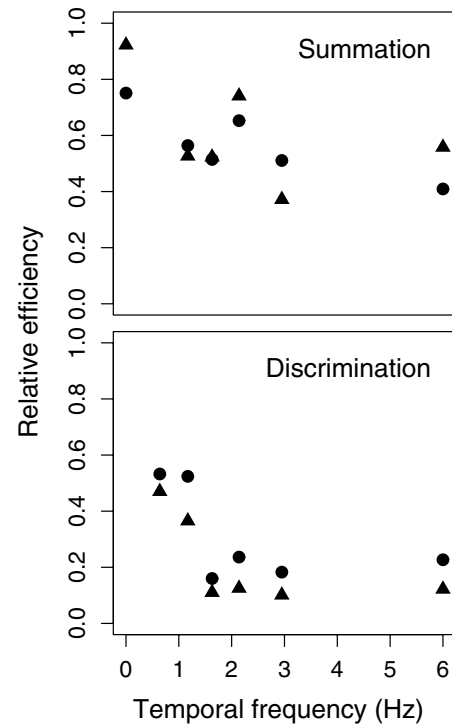


Fig. 5. The sampling efficiency of summation (top) and discrimination (bottom) relative to simple detection plotted as a function of temporal frequency for observers WS (triangles) and HF (circles). In both tasks the relative efficiency declines as speed increases. This may be due to the use of mismatched filters tuned to slow speeds.

Each of the lines in Fig. 3 can be fitted with its own slope and x -intercept according to Eqs. (1)–(3) and thereby give us estimates of internal noise and sampling efficiency in the three tasks. Let us first consider the internal noise or x -intercept. We tested whether the internal noise level differed between the three tasks by comparing the fit of a full model with three x -intercepts to a model having a single x -intercept.

It appears from Fig. 3 that the lines describing the thresholds for each task radiate from a common x -intercept. We performed a likelihood ratio test to see whether the different tasks had statistically different x -intercepts or whether a common x -intercept model fit just as well. A likelihood ratio test (Faraway, 2000, pp. 19–24) found no statistical difference in the fits (HF: $F(21, 23) = 0.029, p = 0.97$; KF: $F(30, 32) = 0.048, p = 0.95$) and so we conclude that there is a source of internal noise that is common to all tasks. For HF this noise (with standard error) has a power spectral density of $0.04 \pm 0.02 \mu\text{s deg}^2$; for KF it is $0.13 \pm 0.03 \mu\text{s deg}^2$. As can be seen from Fig. 3, the common internal noise model with lines radiating from a single x -intercept describes the data well.

It is quite apparent in Fig. 3 that the lines for detection, discrimination, and summation have differing slopes. The slopes do not translate directly into sampling efficiencies because the ideal observer's performance in

discrimination and summation depends on the correlation between the signals. Therefore although the slopes of the discrimination curves for KF and HF look similar, since KF was given slow signals her efficiency (with standard error) is 0.0105 ± 0.0002 whereas HF, who was given faster signals, has an efficiency of only 0.0029 ± 0.0002 . For summation the efficiencies are 0.018 ± 0.007 and 0.015 ± 0.003 for KF and HF respectively. For simple detection the efficiencies are 0.021 ± 0.003 and 0.0104 ± 0.0008 . These efficiencies for detection of a drifting grating are on a par with those found by Eckstein, Whiting, and Thomas (1996). From these results it appears that sampling efficiencies for the three tasks are around 1–2% with the exception of discrimination which may have a very low efficiency for high speeds. For both observers direction discrimination is performed with the lowest efficiency.

Let us now compare the overall pattern of results shown by our real observers in Fig. 3 to those of an ideal observer (Fig. 2). For the ideal observer, changing the speed from 1 to 6 Hz should have pivoted the discrimination curve down below the detection curve, and that did not happen for real observers. In discrimination HF acted as though the correlation between the signals was much higher than it truly was.

The pattern of results in Fig. 3 does not appear very different for observers HF and KF even though they viewed signal pairs with highly different correlations. We examined this result more closely by giving each of three observers the three tasks at two signal speeds. Fig. 4 shows the results for observers HF and KF who viewed a 2 c/deg Gabor that drifted at 1 and 6 Hz; WS viewed an 8 c/deg Gabor. It is clear that a marked change in signal correlation (0 vs 0.77) had little effect on the pattern of results: the 6 Hz data are very similar to the 1 Hz data. When performing direction discrimination of 6 Hz patterns, observers behaved as though the Gabors were much more similar than they truly were.

The fitted lines in each plot in Fig. 4 radiate from a common x -intercept $-N_i$. In each case there was no statistical difference between the common intercept model and one that included separate intercepts for each task. Thus there is a common source of internal noise for simple detection, direction discrimination, and detection of the sum of oppositely moving gratings. For all observers the magnitude of the internal noise was reduced as speed increased from 1 to 6 Hz: for HF the noise declined from 0.13 to $0.04 \mu\text{s deg}^2$, for KF the decline was from 0.20 to $0.13 \mu\text{s deg}^2$, and for WS it declined from 0.18 to $0.07 \mu\text{s deg}^2$.

The sampling efficiencies are near 1–2% for all observers and tasks except for discrimination at 6 Hz. For 1 Hz, the efficiencies for discrimination, summation and detection are: 0.011, 0.013, 0.023 (HF); 0.014, 0.012, 0.012 (KF); 0.022, 0.022, 0.03 (WS). For 6 Hz the efficiencies are: 0.002, 0.012, 0.012 (HF); 0.004, 0.025, 0.012

(KF); 0.003, 0.019, 0.016 (WS). Note how the discrimination efficiency is lowered by about a factor of 5 as the temporal frequency increases from 1 to 6 Hz. This may seem strange when viewing Fig. 4 because the slopes of the discrimination curves for 1 and 6 Hz are about the same. That is precisely the point: for an ideal observer the 6 Hz curve's slope would be dramatically shallower than it is for the real observers (see Fig. 2) and the low sampling efficiency reflects this. Human observers act as though the 6 Hz speed was about the same as 1 Hz.

Why do human observers have such low efficiency in discriminating direction? One possibility is that they use mismatched filters. For example, if they do the 6 Hz discrimination task using spatiotemporal filters tuned to motion at 1 Hz, they will have low efficiency. Perhaps humans can only access filters tuned to low speeds when discriminating direction. If this explanation is correct, then sampling efficiency should systematically decline as the stimulus speed gets faster.

In a second experiment we varied temporal frequency in an effort to see how sampling efficiency varies with speed. We have already seen that the internal noise level is constant across the three tasks at a given speed. Therefore we were able to measure the relative efficiency of discrimination and summation by measuring the energy thresholds for noiseless displays. If we use the notation E_u to represent the energy threshold for the detection of the upwards drifting grating and E_s to represent the threshold for detecting the sum of two oppositely drifting gratings, the threshold ratio

$$\frac{E_u}{E_s} = \frac{N_e + N_i}{k_u} \left(\frac{2k_s(1 + \rho)}{N_e + N_i} \right) = 2(1 + \rho) \frac{k_s}{k_u}$$

can be used to give the ratio of the sampling efficiencies for the two tasks. For a given pair of signals their correlation ρ is known. The relative efficiency of summation is

$$\frac{E_u}{2(1 + \rho)E_s} = \frac{k_s}{k_u}. \quad (4)$$

If E_d represents the threshold for discriminating direction, we can obtain the efficiency of discrimination relative to detection as

$$\frac{E_u}{2(1 - \rho)E_d} = \frac{k_d}{k_u}. \quad (5)$$

The top panel of Fig. 5 plots the efficiency of summation relative to simple detection of a drifting grating as a function of temporal frequency for both observers. The overall tendency is for the relative efficiency to decline as speed increases, although there is a bump of better efficiency at 2 Hz. The same general picture emerges for discrimination in the bottom panel of Fig. 5. The way in which summation and discrimination efficiency both decline with temporal frequency is consistent with the idea that humans have better efficiency for

these tasks at low speeds because they use a pair of templates tuned to low speeds in opposite directions. Such a template pair has a high correlation which would result in good summation and poor discrimination.

In summation and direction discrimination humans act as though the stimuli are slower than they truly are. Such perceptual slowing has been previously observed for low contrast signals like ours (Stone & Thompson, 1992; Thompson, 1982). The perceptual distortion seems to be associated with motion, because previous experiments with static Gabors found summation to be well explained by the cross-correlation between the signals (Manahilov & Simpson, 2001).

5. Conclusions

We compared human performance in the detection, discrimination, and summation of moving gratings to that of an ideal observer. Humans act like an inefficient cross-correlator who adds noise to the stimuli and who wastes a large part of the stimulus energy (Burgess, 1990; Pelli & Farrell, 1999). The data show the presence of a source of internal noise that is common to all three tasks. This noise could be common to all tasks because it occurs early (prior to cross-correlation between stimulus and template for example) or late (due to criterion variability).

Although our analysis which partitions the observers' overall efficiency into sampling efficiency and internal noise is traditional (Bennett, Sekuler, & Ozin, 1999; Burgess & Barlow, 1983; Burgess et al., 1981; Gegenfurtner & Kiper, 1992; Gold, Bennett, & Sekuler, 1999; Kersten, Hess, & Plant, 1988; Nagaraja, 1964; Pardhan, Gilchrist, Elliot, & Beh, 1996), the idea that internal noise can be measured from the threshold-vs-external-noise functions of the type shown in Figs. 2–4 has recently come into question. Kontsevich, Chen, and Tyler (2002) for example emphasize that the “internal noise” as measured in our paradigm depends on both the internal noise level and on transducer nonlinearity. We agree that the interpretation of the measured internal noise is not simple. This problem has long been recognized in our tradition (Legge et al., 1987).

In direction discrimination human sampling efficiency declined markedly at higher speeds. This low efficiency was caused by the observers acting as though the signals were much more correlated than they truly were. This distortion of the signal cross-correlation appears to be caused by the observers using templates of the drifting Gabors that have slower speeds than the actual signals. It not clear what the neural basis of this would be, however. V1 cells function as linear spatiotemporal filters of the required type but these filters are tuned to a wide range of speeds, not just low speeds (Foster, Gaska, Nagler, & Pollen, 1985).

The spatiotemporal distortion introduced by the human visual system may be an inherent flaw, perhaps due to the action of nonlinear units such as V1 complex cells or MT cells. On the other hand, the spatiotemporal distortion may serve some useful purpose in tasks more complex than detection and discrimination of drifting and flickering Gabor patches.

References

- Bennett, P. J., Sekuler, A. B., & Ozin, L. (1999). Effects of aging on calculation efficiency and equivalent noise. *Journal of the Optical Society of America A*, *16*, 654–668.
- Burgess, A., & Barlow, H. B. (1983). The precision of numerosity discrimination in arrays of random dots. *Vision Research*, *23*, 811–820.
- Burgess, A. E. (1990). High level visual decision efficiencies. In C. Blakemore (Ed.), *Vision: Coding and efficiency* (pp. 431–440). New York: Cambridge University Press.
- Burgess, A. E., Wagner, R. F., Jennings, R. J., & Barlow, H. B. (1981). Efficiency of human visual signal discrimination. *Science*, *214*, 93–94.
- Burr, D. C., Ross, J., & Morrone, M. C. (1986). Seeing objects in motion. *Proceedings of the Royal Society of London B*, *227*, 249–265.
- DeAngelis, G. C., Ohzawa, I., & Freeman, R. D. (1993a). Spatiotemporal organization of simple-cell receptive fields in the cat's striate cortex. I. General characteristics and postnatal development. *Journal of Neurophysiology*, *69*, 1091–1117.
- DeAngelis, G. C., Ohzawa, I., & Freeman, R. D. (1993b). Spatiotemporal organization of simple-cell receptive fields in the cat's striate cortex. II. Linearity of temporal and spatial summation. *Journal of Neurophysiology*, *69*, 1118–1135.
- Dobkins, K. R., & Teller, D. Y. (1996). Infant contrast detectors are selective for direction of motion. *Vision Research*, *36*, 281–294.
- Eckstein, M. P., Whiting, J. S., & Thomas, J. P. (1996). Detection and contrast discrimination of moving signals in uncorrelated Gaussian noise. *Society of Photo-optical Instrumentation Engineers Proceedings*, *2712*, 9–25.
- Faraway, J. (2000). *Practical regression and anova using R*. <http://www.stat.lsa.umich.edu/~faraway/book/>.
- Foster, K. H., Gaska, J. P., Nagler, M., & Pollen, D. A. (1985). Spatial and temporal frequency selectivity of neurons in visual cortical areas V1 and V2 of the macaque monkey. *Journal of Physiology*, *365*, 331–363.
- Gegenfurtner, K. R., & Kiper, D. C. (1992). Contrast detection in luminance and chromatic noise. *Journal of the Optical Society of America A*, *9*, 1880–1888.
- Gold, J., Bennett, P. J., & Sekuler, A. B. (1999). Signal but not noise changes with perceptual learning. *Nature*, *402*, 176–178.
- Hamilton, D. B., Albrecht, D. G., & Geisler, W. S. (1989). Visual cortical receptive fields in monkey and cat: spatial and temporal phase transfer function. *Vision Research*, *29*, 1285–1308.
- Kersten, D., Hess, R. F., & Plant, G. T. (1988). Assessing contrast sensitivity behind cloudy media. *Clinical Vision Science*, *2*, 143–158.
- Kontsevich, L. L., Chen, C.-C., & Tyler, C. W. (2002). Separating the effects of response nonlinearity and internal noise psychophysically. *Vision Research*, *42*, 1771–1784.
- Legge, G., Kersten, D., & Burgess, A. E. (1987). Contrast discrimination in noise. *Journal of the Optical Society of America A*, *4*, 391–406.
- Levinson, E., & Sekuler, R. (1975). The independence of channels in human vision selective for direction of movement. *Journal of Physiology*, *250*, 347–366.
- Levitt, H. (1971). Transformed up-down methods in psychoacoustics. *Journal of the Acoustical Society of America*, *49*, 467–477.

- Manahilov, V., & Simpson, W. A. (2001). Energy model for contrast detection: spatial-frequency and orientation selectivity in grating summation. *Vision Research*, *41*, 1547–1560.
- Marsaglia, G. (1994). Yet another rng. Posted to internet newsgroup sci.stat.math.
- McLean, J., & Palmer, L. A. (1989). Contribution of linear spatio-temporal receptive field structure to velocity selectivity of simple cells in area 17 of cat. *Vision Research*, *29*, 675–679.
- McLean, J., & Palmer, L. A. (1994). Organization of simple cell responses in the three-dimensional (3-D) frequency domain. *Visual Neuroscience*, *11*, 295–306.
- McLean, J., Raab, S., & Palmer, L. A. (1994). Contribution of linear mechanisms to the specification of local motion by simple cells in areas 17 and 18 of the cat. *Visual Neuroscience*, *11*, 271–294.
- Nagaraja, N. S. (1964). Effect of luminance noise on contrast thresholds. *Journal of the Optical Society of America*, *54*, 950–955.
- Pardhan, S., Gilchrist, J., Elliot, D. B., & Beh, G. K. (1996). A comparison of sampling efficiency and internal noise level in young and old subjects. *Vision Research*, *36*, 1641–1648.
- Pelli, D. G. (1990). The quantum efficiency of vision. In C. Blakemore (Ed.), *Vision: Coding and efficiency* (pp. 3–24). New York: Cambridge University Press.
- Pelli, D. G., & Farrell, B. (1999). Why use noise? *Journal of the Optical Society of America A*, *16*, 647–653.
- Pelli, D. G., & Zhang, L. (1991). Accurate control of contrast on microcomputer displays. *Vision Research*, *31*, 1337–1350.
- Reid, R. C., Victor, J. D., & Shapley, R. M. (1997). The use of m-sequences in the analysis of visual neurons: linear receptive field properties. *Visual Neuroscience*, *14*, 1015–1027.
- Reisbeck, T. E., & Gegenfurtner, K. R. (1999). Velocity tuned mechanisms in human motion processing. *Vision Research*, *39*, 3267–3285.
- Simpson, W. A., & Manahilov, V. (2001). Matched filtering in motion detection and discrimination. *Proceedings of the Royal Society of London B*, *268*, 703–709.
- Stone, L. S., & Thompson, P. (1992). Human speed perception is contrast dependent. *Vision Research*, *32*, 1535–1549.
- Stromeyer, C. F., III, Madsen, J. C., Klein, S., & Zeevi, Y. Y. (1978). Movement-selective mechanisms in human vision sensitive to high spatial frequencies. *Journal of the Optical Society of America*, *68*, 1002–1005.
- Thiele, A., Dobkins, K. R., & Albright, T. D. (2000). Neural correlates of contrast detection at threshold. *Neuron*, *26*, 715–724.
- Thompson, P. (1982). Perceived rate of movement depends on contrast. *Vision Research*, *22*, 377–380.
- Watson, A. B., Thompson, P. G., Murphy, B. J., & Nachmias, J. (1980). Summation and discrimination of gratings moving in opposite directions. *Vision Research*, *20*, 341–347.
- Watson, A. B., & Turano, K. (1995). The optimal motion stimulus. *Vision Research*, *35*, 325–336.
- Whalen, A. D. (1971). *Detection of signals in noise*. New York: Academic Press.